scientific reports

Check for updates

OPEN

Photoreceptor regeneration occurs normally in microglia-deficient *irf8* mutant zebrafish following acute retinal damage

Ping Song[1], Dhwani Parsana[1], Rupesh Singh[1], Lana M. Pollock[1], Bela Anand-Apte[1,2,3] & Brian D. Perkins[1,2,3]✉

Microglia are resident immune cells in the central nervous system, including the retina that surveil the environment for damage and infection. Following retinal damage, microglia undergo morphological changes, migrate to the site of damage, and express and secrete pro-inflammatory signals. In the zebrafish retina, inflammation induces the reprogramming and proliferation of Müller glia and the regeneration of neurons following damage or injury. Immunosuppression or pharmacological ablation of microglia reduce or abolish Müller glia proliferation. We evaluated the retinal architecture and retinal regeneration in adult zebrafish *irf8* mutants, which have significantly depleted numbers of microglia. We show that *irf8* mutants have normal retinal structure at 3 months post fertilization (mpf) and 6 mpf but fewer cone photoreceptors by 10 mpf. Surprisingly, light-induced photoreceptor ablation induced Müller glia proliferation in *irf8* mutants and cone and rod photoreceptor regeneration. Light-damaged retinas from both wild-type and *irf8* mutants show upregulated expression of *mmp-9*, *il8*, and *tnf8* pro-inflammatory cytokines. Our data demonstrate that adult zebrafish *irf8* mutants can regenerate normally following acute retinal injury. These findings suggest that microglia may not be essential for retinal regeneration in zebrafish and that other mechanisms can compensate for the reduction in microglia numbers.

Keywords Microglia, Regeneration, Retina, Photoreceptors, Müller glia, Inflammation

Unlike mammals, zebrafish possess the remarkable capacity for endogenous regeneration in response to acute retinal damage[1–3]. Retinal injury induces a reprogramming event within a population of Müller glia and these cells adopt a state similar to retinal progenitors. The reprogrammed Müller glia re-enter the cell cycle and undergo asymmetric cell divisions to produce neuronal progenitor cells (NPCs). The NPCs amplify through additional cell divisions and migrate to the site of injury where they differentiate to replace lost neurons[3–5].

The successful regeneration of lost neurons in the zebrafish retina depends on the proper control of inflammatory signaling. Retinal injury triggers the release of several inflammatory cytokines and growth factors[2,6–8]. Müller-glia derived NPCs release leptin and IL-6 family cytokines including *il-11a, il-11b, clcf1*, and *crlf1a*[7]. Microglia also upregulate expression of several inflammatory cytokines, including *il1b, tnfa, tnfb*, and *granulin-1*, and *-2*[9]. Many of these pro-inflammatory cytokines are necessary for Müller glia reprogramming and the proliferation of NPCs[6,7]. Additional evidence that inflammation initiates regeneration comes from the use of the glucocorticosteroid dexamethasone to pharmacologically suppress inflammation prior to retinal damage. Dexamethasone reduces or abolishes the proliferation of Müller glia and neuronal progenitors in adult zebrafish[8,10–12]. While inflammation is necessary to initiate Müller glia proliferation, resolving the inflammatory response must occur to ensure accurate regeneration. Matrix metalloproteinase-9 (Mmp-9) is an enzyme secreted by Müller glia that cleaves cytokines to resolve inflammation following injury[8]. In the absence of Mmp-9, Müller glia hyperproliferate and overproduce new photoreceptors in response to injury; however, the regenerated cone photoreceptors rapidly degenerate due to excessive inflammation[8]. Collectively, these data support a model where dynamic inflammatory signaling initiates and ensures successful regeneration.

[1]Department of Ophthalmic Research, Cole Eye Institute, Cleveland Clinic, Cleveland, OH, USA. [2]Department of Ophthalmology, Cleveland Clinic Lerner College of Medicine, Case Western Reserve University, Cleveland, OH, USA. [3]Department of Molecular Medicine, Cleveland Clinic Lerner College of Medicine, Case Western Reserve University, Cleveland, OH, USA. ✉email: perkinb2@ccf.org

Microglia constitute the primary resident immune cell in the central nervous system, including the vertebrate retina[13]. In the healthy adult retina, microglia adopt a ramified morphology and are distributed in a planar fashion within the outer and inner plexiform layers to survey retinal synapses. Microglia are highly specialized macrophages that play several crucial roles within the adult retina, including maintaining synaptic integrity and contributing to the processing of cone-driven visual information[14]. Depletion of microglia results in decreased electroretinogram (ERG) responses and synapse loss in mice, indicating microglia provide neurotrophic support for synapse maintenance[15].

In the diseased CNS, microglia react to an ever-changing environment that includes apoptotic cells and cellular debris, protein aggregates or plaques, and changes in extracellular ATP or superoxide production[16,17]. In response to these stimuli, microglia adopt new states that are defined by the transcriptional and proteomic profiles, morphology, and motility[17]. How microglia function will depend on the state of a particular population. This may include the release of pro-inflammatory cytokines, such as TNFα and IL1β, and phagocytosis of synapses and cellular debris, or the release of anti-inflammatory cytokines such as IL10 to prevent neuronal death[17,18]. In response to inherited retinal degeneration or photoreceptor injury, microglia initially respond to photoreceptor death by transitioning from a ramified to amoeboid morphology. In humans with retinal disease and mouse models of inherited retinal degeneration, microglia migrate from the plexiform layers to the outer nuclear layer and subretinal space[14,19]. Historically termed "activated microglia", these cells proliferate and show dynamic changes in gene expression. In response to injury or damage microglia initially downregulate homeostatic genes and begin secreting pro-inflammatory proteins[9,14]. Microglia subsequently adopt a protective role and downregulate genes associated with immune response pathways while upregulating antioxidant pathway genes[14]. Evidence suggests that precise regulation of this dynamic inflammatory response plays a central role in the repair and regeneration of damaged or diseased tissues[2,20–22].

While microglia represent a significant source of pro-inflammatory signals that can induce regeneration, the function and necessity of microglia during regeneration have not been fully resolved. In zebrafish, both transgenic and pharmacological depletion of macrophage–microglia populations suppressed retinal regeneration. Adult zebrafish continuously treated with the CSF1R inhibitor PLX3397 prior to, and following laser-induced photoreceptor ablation showed no evidence of retinal regeneration[23]. In larval zebrafish, the kinetics of regeneration were significantly delayed following metronidazole (MTZ)-induced co-ablation of rods and microglia in *Tg*(*rho:NTR-YFP;mpeg1:NTR-YFP*) double transgenic zebrafish[24]. In contrast, PLX5562-mediated depletion of microglia in the mouse retina resulted in significantly more Müller glia-derived neurons following NMDA damage and *Ascl1* overexpression, suggesting that microglia suppress regeneration in mammals[25]. Given the centrality of microglia to the inflammatory response, it is important to consider different microglia depletion models and how this may impact the results of regeneration studies.

Here, we utilized the zebrafish *irf8* mutant to investigate retinal regeneration in a genetic model of microglia deficiency[26]. The Interferon regulatory factor 8 (Irf8) is a transcription factor that plays a critical role in macrophage/monocyte fate and IRF8 deficiency in human, mouse, and zebrafish leads to a complete loss of embryonic macrophages[26] and a significant reduction in macrophages and microglia in the CNS of adult zebrafish[27]. We confirmed that zebrafish *irf8* mutant adults had a significant reduction in retinal microglia and find that older adults show reduced cone numbers. Unexpectedly, we found that photoreceptor degeneration caused by high-intensity light damage or genetically-induced photoreceptor ablation triggered a robust regeneration response from Müller glia in *irf8* mutants and that the inflammatory transcriptional response was similar between wild-type and *irf8* mutants. Taken together, these results suggest that microglia are not essential for pro-inflammatory signaling necessary to induce regeneration in the zebrafish retina.

Materials and methods

Animal maintenance

Adult zebrafish were housed in 3 L and 10 L tanks in an Aquatic Habitats recirculating system (Pentair; Apopka, FL, USA) with a 14:10 light–dark cycle and fed brine shrimp and commercial flake food. Zebrafish lines utilized in this study included the mutant line[26] *irf8*^{st95}, the transgenic line *Tg*(*rho:YFP-Eco.NfsB*)*gmc500* (herein referred to as *Tg*(*rho:ntr-YFP*)) used to ablate rod photoreceptors[28], and the transgenic line *Tg*(*-3.5fabp10a:gc-EGFP*)*lri500* (previously and herein referred to as *Tg*(*l-fabp:DBP-eGFP*)) to assess blood-retinal-barrier (BRB) permeability[29]. Animals from *irf8* lines were genotyped using high resolution melt analysis (HRMA) using specified primer sets (Extended Data Table 1-1). Homozygote, heterozygote, and wild-type siblings were identified for each cross. Transgenic lines were confirmed by PCR using primers specific for GFP or *nfsB* (Extended Data Table 1-1). Experiments included animals of both sexes and were used at the specified ages. All experiments involving animals were approved by the Institutional Animal Care and Use Committee (IACUC) at the Cleveland Clinic and in accordance with relevant guidelines and regulations, including the ARVO statement for the use of animals in research and the ARRIVE guidelines.

EdU labeling

To label proliferating cells, animals were anesthetized with tricaine methanesulfonate (0.4 mg/mL) and placed on a wet towel and injected intraperitoneally with 20 µL of a 20 mM EdU solution (PBS). Animals were injected and allowed to recover for the specified time period prior to euthanasia and enucleation. Eyes were subsequently processed for immunohistochemistry as described.

Immunohistochemistry

Adult zebrafish were euthanized by immersion in ice-cold water for 5 min and decapitated with a razor blade. Eyes were rapidly enucleated, immersed overnight in 4% paraformaldehyde/5% sucrose/0.8× PBS. Samples were

equilibrated through 3 washes in 5% sucrose/0.8× PBS for a total of 3 h at room temperature and transferred to 30% sucrose/0.8× PBS for at least 3 h at room temperature. Eyes were washed in a 1:1 solution of PolarStat Plus and 30% sucrose/0.8× PBS for a minimum of 8–10 h at 4 °C. Eyes were then embedded for cryosectioning or stored at − 80 °C until sectioning.

Transverse cryosections sections (10 µm) were cut and mounted on Superfrost Plus slides and dried at room temperature overnight. Slides were washed 3 × 10 min in 0.8× PBS and then incubated in blocking solution (0.8× PBS + 2% BSA, 5% normal goat serum, 0.1% Tween-20, 0.1% DMSO) for 1 h. The following primary antibodies were used: mouse monoclonal Zpr1 (1:100, Zebrafish International Resource Center (ZIRC), Eugene, OR, USA), mouse monoclonal Zpr3 (1:200, ZIRC), mouse monoclonal 4C4 (1:1000), rabbit polyclonal L-plastin (1:1000, GeneTex, Irvine, CA, USA, GTX124420), rabbit polyclonal anti-GFP (1:500, Life Technologies, Carlsbad, CA, USA, A11122), mouse monoclonal PCNA (1:500, Sigma, St. Louis, MO, USA, clone PC-10), peanut agglutinin (PNA)-lectin conjugated to Alexa-568 (1:100, ThermoFisher, Waltham, MA, USA). EdU labeling was detected with the Click-iT Edu Alexa Fluor-555 Imaging Kit (ThermoFisher). Alexa-conjugated secondary antibodies were used at 1:500 in blocking buffer and incubated for at least 1 h. Slides were counterstained with 4,5-diamidino-2-phenylindole (DAPI) to stain nuclei.

Light damage

Light damage experiments were performed using a protocol as previously described[10,30]. Adult zebrafish were first dark adapted for up to 18 h. Animals were placed in a 250 mL glass beaker with system water that was seated inside a 1 L glass beaker with Milli-Q water. Animals were exposed to high-intensity light from a 120 W X-CITE series 120Q metal halide lamp (Excelitas) for 50 min and then exposed to 14,000 lx light from an illumination cage for 5 h. Animals were allowed to recover in system water for up to 30 days prior to enucleation.

Image acquisition and quantification

Projection images (z-stacks; 5–10 µm) of immunostained cryosections were obtained on a Zeiss Imager Z.2 equipped with an ApoTome using 10× dry or 20× dry lenses (Zeiss). Images were acquired with Zen2 software and post-processed in ImageJ. All imaging and quantitative analysis was performed on dorsal retina sections, which contained or were immediately adjacent to the optic nerve. Quantification was performed manually. Cell or staining densities were calculated by measuring the curvilinear distance of retina in each section using ImageJ. Each data point represents the ratio or density from the dorsal region of a central retinal section from one eye.

Metronidazole treatment

To ablate photoreceptors using the *Tg*(*rho:ntr-YFP*) line, adult zebrafish were incubated in system water containing 10 mM metronidazole (Sigma) for 24 h in a 28 °C incubator. Animals were transferred to fresh system water and allowed to recover for 48 h prior to euthanasia. The eyes were removed and processed as described above.

N,N-diethylaminobenzaldehyde (DEAB) treatments

Tg(*l-fabp:DBP-eGFP*) adult fish at 6 mpf were placed in system water containing 5 µM DEAB and 0.6% DMSO for up to 48 h and evaluated for vascular breakdown as previously described[31].

Confocal scanning laser ophthalmoscopy (cSLO) imaging

cSLO instrumentation and imaging was performed as previously described[32] with a SPECTRALIS ophthalmascope (Heidelberg Engineering) used for all imaging. Briefly, adult animals were anesthetized with buffered tricaine and placed in a custom holder[33].

qRT-PCR

Light damage treatments were conducted on 6 mpf *irf8* mutants and wild-type siblings (n = 6) as described above. Following light exposure, animals were allowed to recover for 6 h post injury (hpi), 48 hpi, 72 hpi, or 1 week post injury and subsequently euthanized. Except for the 6 hpi time point, animals were dark adapted for 24 h prior to euthanasia. Retinas were rapidly dissected in sterile 0.8× PBS, separated from the RPE, and flash frozen in a methanol/dry ice bath. For each time point, a total of 4 biological samples, each containing 3 pooled retinas, were collected (12 total retinas per genotype). RNA was extracted using Trizol and chloroform and precipitated with isopropanol using GlycoBlue as a co-precipitant. The resulting RNA was resuspended in nuclease-free water, treated with DNase and precipitated with LiCl and isopropanol and GlycoBlue. The purified RNA was resuspended in nuclease-free water. The yield and purity was assessed by TapeStation and Qubit analysis at the Lerner Research Institute Genomics Core. A total of 500 ng of purified RNA was used for reverse transcription and qPCR. Reverse transcription and qPCR were done per manufacturer's instructions using the Bio-Rad iScript cDNA synthesis kit and the Bio-Rad SsoFast EvaGreen Supermix kit, respectively. Reactions were run on a Bio-Rad CFX96 Touch Real-Time PCR detection system and analyzed using CFX Manager. Primer sequences are listed in Extended Data Table 1-1. For qPCR reactions, 3 technical replicates were performed on all 4 biological samples. Fold changes were calculated by the ΔΔC(t) method, with 18S rRNA used for normalization.

Statistics and data analysis

All data was analyzed and graphed using GraphPad Prism (v8). Data sets were first tested for normal distribution using Prism. Normally distributed data sets were subsequently analyzed by Student's *t*-tests with Welch's correction or one-way ANOVA with Dunnet T3 correction for multiple comparisons. Where necessary, non-parametric Kruskal–Wallis tests were used.

Results

Zebrafish *irf8* mutants have reduced numbers of microglia but normal retinal architecture

We investigated the role of microglia in the adult zebrafish retina using the *irf8*^{st95} mutant, which is a null allele resulting from a frameshift deletion located three amino acids 3′ from the translation start codon[26]. Adult *irf8* mutants were reported to have a significant reduction in macrophages and microglia in the CNS[27] and we previously noted reduced numbers of 4C4+ microglia in retinal flat-mounts of adult retinas[10]; however, the long-term consequences of microglia depletion in the zebrafish retina remains undescribed. Microglia were stained with the monoclonal antibody 4C4, which recognizes the protein encoded by the microglia-specific gene *galectin 3 binding protein b* (*lgals3bpb*)[34], and the pan-leukocyte marker L-plastin (Lcp1). In wild-type retinas, microglia reside in the subretinal space (SRS) between the photoreceptor outer segments and the retinal pigment epithelium (RPE), the outer plexiform layer (OPL), and the proximal and distal surfaces of the inner plexiform layer (IPL). All 4C4+ cells colocalized with L-plastin (Fig. 1A). We next quantified the number and location of 4C4+ microglia in transverse retinal sections of zebrafish at 3 months post fertilization (mpf), 6 mpf, and 10 mpf (Fig. 1B). At 3 mpf, the *irf8* mutants had 80% fewer microglia in the IPL as compared to wild-type siblings (1.83 ± 1.6 vs. 9.06 ± 4.1 4C4+ cells/1000 µm; $p \leq 0.005$). At both 6 mpf and 10 mpf, *irf8* mutants had 70% fewer microglia in the IPL compared to wild-type siblings (2.5 ± 1.8 vs. 7.9 ± 2.2; $p \leq 0.05$ and 3.1 ± 3.5 vs. 10.4 ± 3.5; $p \leq 0.005$ 4C4+ cells/1000 µm, respectively) (Fig. 1C). Within the OPL, the *irf8* mutants had 63% fewer microglia at 3 mpf compared to wild-type siblings (4.4 ± 1.4 vs. 11.7 ± 2.5; $p \leq 0.0001$), 50% fewer microglia at 6 mpf (5.6 ± 3.3 vs. 11.0 ± 4.1; $p \leq 0.05$) and 54% fewer microglia at 10 mpf (6.5 ± 3.6 vs. 14.1 ± 3.3; $p \leq 0.005$) (Fig. 1D). In the SRS, the *irf8* mutants had 77% fewer microglia than wild-type siblings at 3 mpf (3.1 ± 2.9 vs. 13.1 ± 2.9; $p \leq 0.0001$), and 6 mpf (2.6 ± 1.9 vs. 11.1 ± 4.0; $p \leq 0.0005$) and 65% fewer microglia at 10 mpf (5.8 ± 4.2 vs. 16.4 ± 6.5; $p \leq 0.05$) (Fig. 1E). When comparing the overall number of microglia in transverse sections, the *irf8* mutants had 75% fewer microglia than wild-type siblings at 3 mpf (9.1 ± 4.8 vs. 35.8 ± 6.8; $p \leq 0.0001$), 65% fewer microglia at 6 mpf (10.6 ± 4.5 vs. 30.0 ± 5.6; $p \leq 0.0001$) and 60% fewer microglia at 10 mpf (16.2 ± 9.4 vs. 40.8 ± 10.3; $p \leq 0.005$) (Fig. 1E). Although the number of microglia varied among individual animals, no statistically significant age-dependent changes were found in either wild-type animals or *irf8* mutants. Taken together, the data indicate that *irf8* mutants showed a 50–80% reduction in microglia density throughout the retina, with

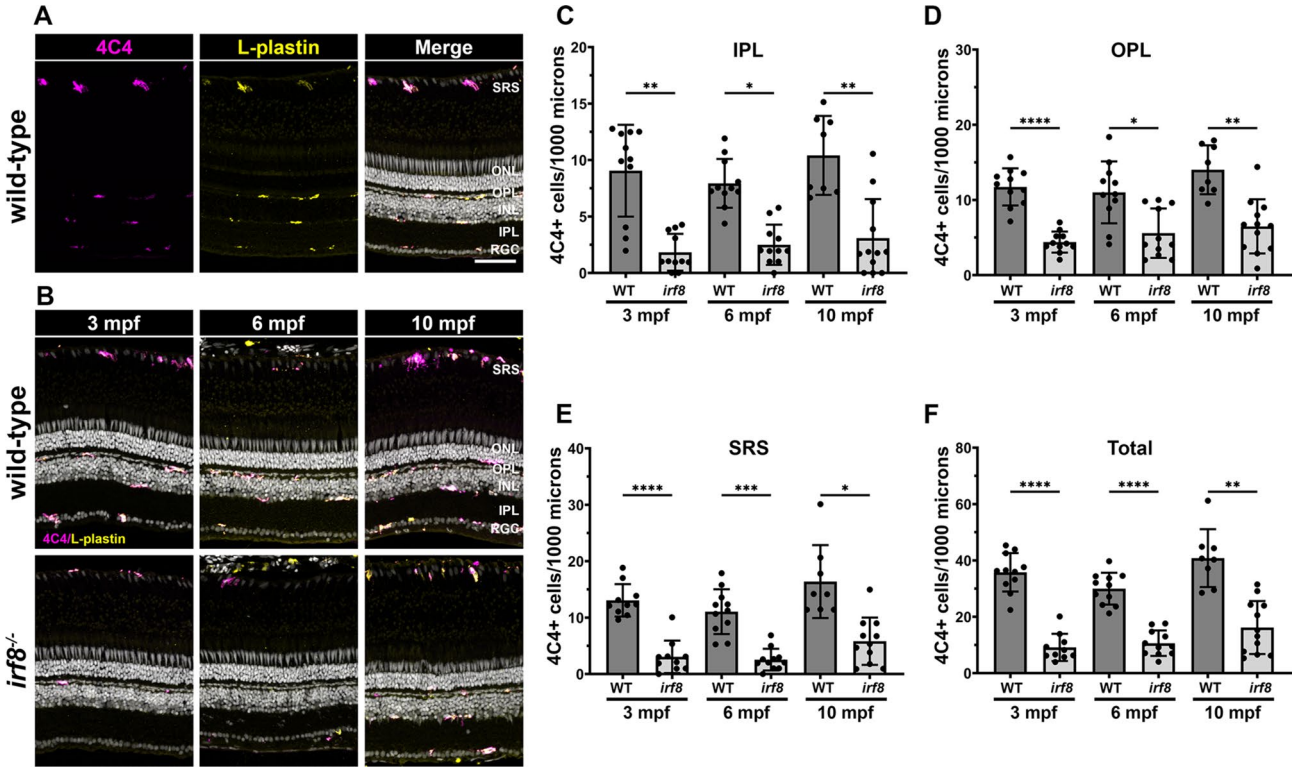

Fig. 1. Adult *irf8* mutants have a significantly fewer retinal microglia. (**A**) 4C4 (magenta) and L-plastin (yellow) immunoreactivity in 6 mpf wild-type retinas to label microglia. (**B**) Immunohistochemistry of 3 mpf, 6 mpf, and 10 mpf wild-type (top row) and *irf8* mutants (bottom row) with 4C4 (magenta) and L-plastin (yellow). (**C**–**F**) Quantification of 4C4+ cells in the inner plexiform layer (IPL) outer plexiform layer (OPL), subretinal space (SRS), and total retina of wild-type and *irf8* mutants with age. Data are plotted as means ± SD and p-values were generated by Welch's ANOVA test with Dunnett's T3 multiple comparisons test (ONL, SRS, total) or Kruskal–Wallis test with Dunn's correction for multiple comparisons (INL). *$p < 0.05$, **$p < 0.01$, ***$p < 0.005$, ****$p < 0.0001$. *SRS* subretinal space, *ONL* outer nuclear layer, *OPL* outer plexiform layer, *INL* inner nuclear layer, *IPL* inner plexiform layer, *RGC* retinal ganglion cell layer. Scale bars, 50 µm (**A**,**B**).

the greatest reduction seen in the IPL and SRS. Furthermore, in both wild-type and *irf8* animals, the number of microglia does not significantly change with age.

Microglia provide neurotrophic support to the developing CNS and maintain homeostasis and normal synaptic function in the uninjured retina. Retinal structure and retinal thickness were not impacted by sustained depletion of microglia; however, significant deficits in the electroretinograms (ERG) a-wave and b-wave responses correlated with synaptic degeneration in the outer plexiform layer of mice lacking microglia[15]. To determine if reduced microglial numbers influenced retinal structure in zebrafish, we compared cone density in *irf8* mutants and wild-type siblings at different ages (Fig. 2A–F). We quantified both cone outer segments using peanut agglutinin (PNA) and cone inner segments and cell bodies with the monoclonal antibody Zpr1 (Fig. 2G,H). Cone density in *irf8* mutants was comparable to that of wild-type animals at both 3 mpf and 6 mpf. At 10 mpf, however, cone density was reduced by 15% in the *irf8* mutants compared to wild-type siblings (207.5 ± 24 vs. 242.7 ± 10.4 Zpr1+ cones/1000 µm; $^{**}p < 0.01$). When PNA+ cone outer segments (COS) were quantified, 35% fewer were found in *irf8* mutants (97.9 ± 48.7 vs 150.5 ± 48.8 PNA+ COS/1000 µm; $^{*}p < 0.05$) although greater

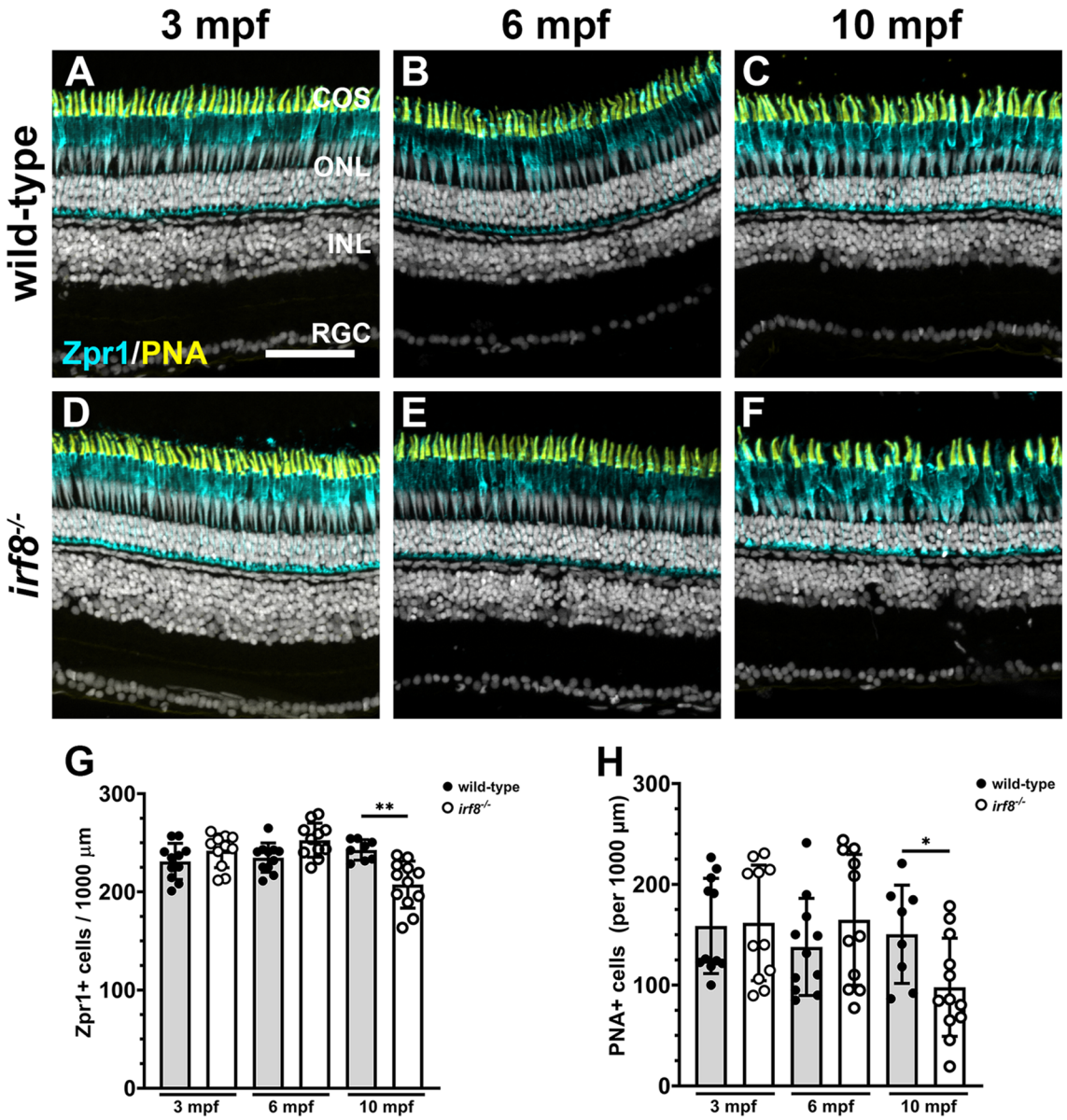

Fig. 2. Cone photoreceptors degenerate in 10 mpf adult *irf8* mutants. (**A**–**F**) Immunohistochemistry with Zpr1 (magenta) and peanut agglutinin (PNA; yellow) on retinal cryosections from wild-type (**A**–**C**) and *irf8* mutants (**D**–**E**) at 3 mpf, 6 mpf, and 10 mpf. (**G**) Quantification of Zpr1+ cell density in the dorsal retina of wild-type and *irf8* mutants with age. (**H**) Quantification of PNA+ cone outer segments in the dorsal retina of wild-type and *irf8* mutants with age. Data are plotted as means ± SD and p-values were generated by Welch's ANOVA test with Dunnett's T3 multiple comparisons test (Zpr1) or an unpaired *t*-test (PNA). $^{*}p < 0.05$, $^{**}p < 0.01$. *COS* cone outer segments, *ONL* outer nuclear layer, *INL* inner nuclear layer, *RGC* retinal ganglion cell layer. Scale bar, 50 µm.

variation existed between samples in both wild-type and *irf8* groups. From these results, we conclude that the loss of microglia leads to a slow, but progressive loss of cone photoreceptors.

Wild-type and *irf8* mutant retinas at different ages were immunostained with an anti-PCNA antibody to label proliferating cells (Fig. 3A–F). PCNA+ cells were quantified in the outer nuclear layer (ONL) to assess proliferation of rod progenitors (Fig. 3G), and the inner nuclear layer (INL), which should measure proliferation of Müller glia (Fig. 3H). We observed similar numbers of proliferating rod progenitors in the ONL when comparing wild-type animals to *irf8* mutants (Fig. 3G). The number of proliferating cells in the ONL was highest at 3 mpf, likely due to ongoing growth of the eye and retina, which slows as the fish ages[35]. Few PCNA+ cells were observed in the ONL at 6 mpf or 10 mpf and no statistical difference was found between wild-type or *irf8* mutants. Very few PCNA+ cells in the INL Müller glia were observed at 3 mpf and 6 mpf in wild-type or *irf8* mutants. At 10 mpf, however, a significant increase in PCNA+ cells in the INL was found in *irf8* mutants as compared to wild-type siblings (Fig. 3H). This correlated with the age when cone loss was observed (Fig. 2), although the number of inflammatory cells remained limited and did not increase in *irf8* mutants (Fig. 1). Overall, there was no significant difference in the total number of PCNA+ cells between wild-type and *irf8* mutant (Fig. 3I), although a difference was seen in the number of PNCA+ cells in the INL (Fig. 3H). Taken together, these results suggested that the

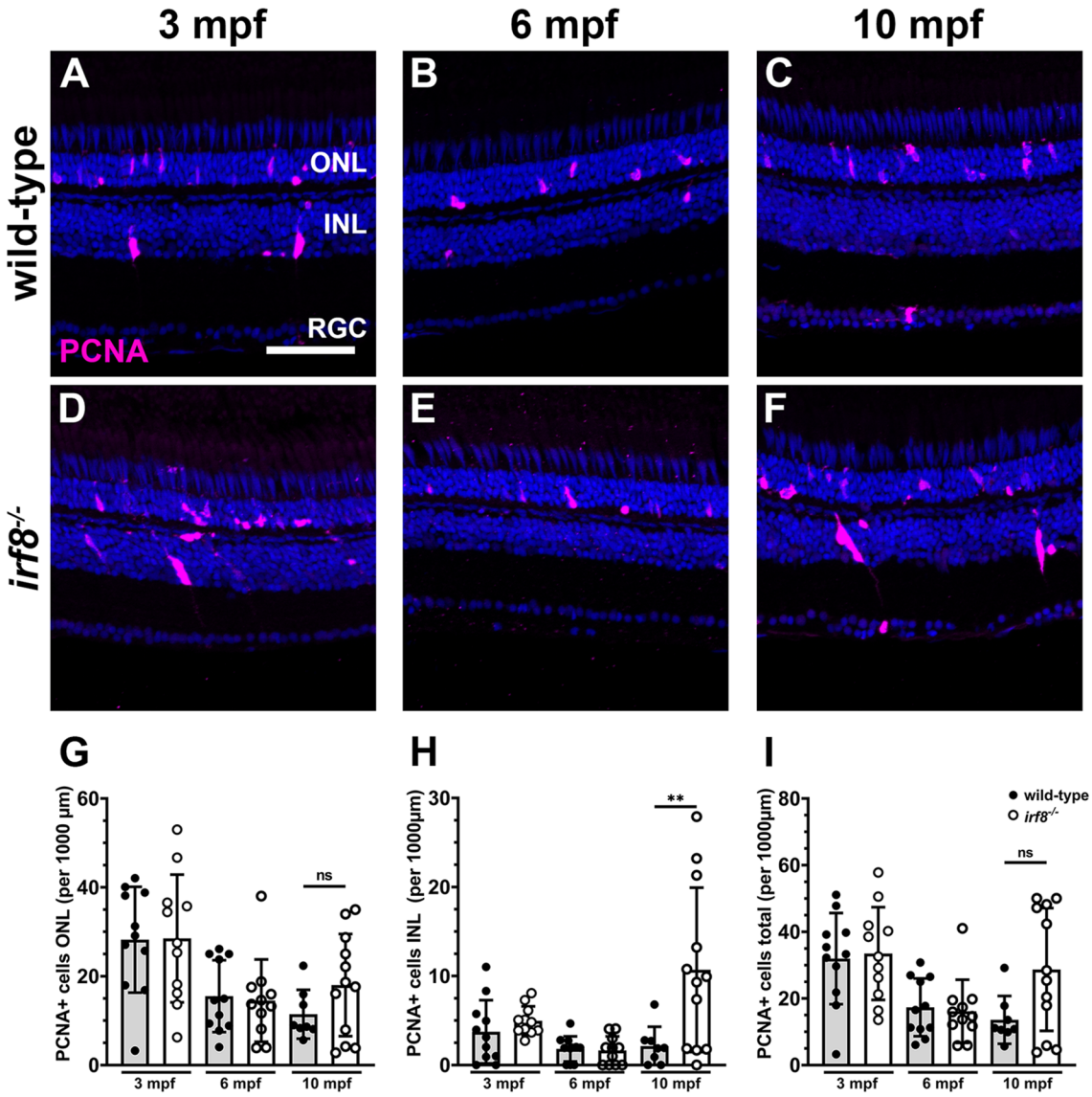

Fig. 3. Proliferation of cells in the INL increases in 10 mpf *irf8* mutants. (**A**–**F**) Immunohistochemistry with anti-PCNA antibodies (magenta) on retinal cryosections from wild-type (**A**–**C**) and *irf8* mutants (**D**,**E**) at 3 mpf, 6 mpf, and 10 mpf. (**G**–**I**) Quantification of PCNA+ cell density in the ONL, INL, and total PCNA density of wild-type and *irf8* mutants with age. Data are plotted as means ± SD and individual points represent data from one retina (n = 8–12). All data were assessed for normal distributions and equal standard deviations. All p-values were generated by unpaired *t*-tests or unpaired *t*-tests with Welch's correction; $^{**}p < 0.01$. *ONL* outer nuclear layer, *INL* inner nuclear layer, *RGC* retinal ganglion cell layer. Scale bar, 50 µm.

microglia deficiency in *irf8* mutants leads to cone loss in older animals and this induced a modest regenerative response involving Müller glia proliferation.

Acute light damage induces proliferation of Müller glia and regeneration of photoreceptors in *irf8* mutants

In response to damage, microglia release a number of pro-inflammatory cytokines[9] and microglia are believed to be necessary for Müller glia-dependent regeneration following both acute injury and in chronic retinal degeneration[2,23]. Experimental ablation of microglia or pre-treatment with the anti-inflammatory steroid dexamethasone prior to acute retinal injury significantly reduces the number of proliferating Müller glia and prevents retinal regeneration[8,11,23,24]. To determine if zebrafish *irf8* mutants would show a similar deficiency in injury-induced Müller glia proliferation, photoreceptors in 6 mpf *irf8* mutants and wild-type siblings were ablated by high-intensity light and retinas were stained with anti-PCNA antibodies at 24, 48, and 72 h post injury (hpi) (Fig. 4A,B). At 24 hpi, a small number of PCNA+ cells were observed in both the INL and ONL of wild-type retinas, consistent with proliferation of both Müller glia and rod precursor cells (Fig. 4A). The number of PCNA+ cells increased in the INL and ONL at 48 hpi and by 72 hpi, columns of proliferating precursors were found in the INL. Surprisingly, PCNA+ cells were observed in a similar pattern in the INL and ONL of *irf8* mutants following light damage (Fig. 4B). When the number of PCNA+ cells were quantified in the INL, ONL, and full retina at 24, 48, and 72 hpi, no statistical difference was found between wild-type and *irf8* mutants (Fig. 4C–E).

To determine if the Müller glia-derived progenitors could differentiate and regenerate photoreceptors, 6 mpf wild-type and *irf8* mutants were light-damaged and allowed to recover for 1 month. To mark the area of regeneration, animals were injected with EdU at 48 hpi and subsequently assessed for proliferation at 3 days post injury (dpi) or stained with Zpr1 and PNA at 30 dpi (see also[10] for details). At 3 dpi, light damage had ablated cones in the dorsal retina and a number of EdU+ proliferating progenitors were observed in the INL of both wild-type and *irf8* mutants (Fig. 5A,B; middle row). After 30 dpi, cones had fully regenerated and the Müller glia-derived progenitors that had migrated to the ONL and differentiated into photoreceptors were labeled with EdU. Light damage ablates photoreceptors in the central region of the dorsal retina, leaving the peripheral retina undamaged and providing an internal control of pre-lesion cone densities[10,36]. Cone densities were quantified in the damaged and undamaged areas of wild-type and *irf8* mutants at 30 dpi. Cone density was similar between the regenerated (i.e. "damaged") region and undamaged region in both wild-type animals and *irf8* mutants (Fig. 5C). Importantly, the number of regenerated cones was similar between wild-type and *irf8* mutants. Taken together, these data indicate that microglia deficiency did not affect the generation of Müller glia-derived progenitors or the subsequent regeneration of cone photoreceptors in *irf8* mutants.

The robust damage-induced photoreceptor regeneration observed in *irf8* mutants led us to ask whether light damage triggered proliferation of microglia. Immediately following light damage, *irf8* mutants and wild-type siblings were injected with EdU and eyes were collected 24 hpi. To identify cells that actively passed through S-phase between 24–48 hpi and 48–72 hpi, animals were given a single injection of EdU at 24 hpi or 48 hpi and subsequently collected the following day. Retinal sections were co-labeled with EdU and 4C4 to identify microglia (4C4+) that underwent proliferation in the previous 24 h. As the vast majority of 4C4+ cells were located in the subretinal space (SRS) at all time points, quantification of 4C4+ and EdU+ cells was limited to those found within the SRS (Fig. 6). At 24 hpi, less than one EdU+ cell on average was seen in the SRS of either wild-type or *irf8* mutants (Fig. 6A,D,G). Microglia were 3.5-fold more abundant in the SRS of wild-type retinas compared to *irf8* mutants at 24 hpi (Fig. 6H). By 48 hpi, the number of EdU+ cells in the SRS of wild-type animals was 13-fold higher than that of *irf8* mutants (Fig. 6G; 74.8 ± 11.6 vs 5.6 ± 2.6). Between 24 and 48 hpi the number of 4C4+ cells in the SRS increased significantly by approximately twofold in wild type retinas (43.8 ± 14 vs. 90 ± 12.7; $p < 0.02$) but was not significantly increased in *irf8* mutants (12.5 ± 5.6 vs 19.8 ± 6.9) during the same period. Moreover, the number of 4C4+ cells were 4.5-fold higher in wild-type compared to *irf8* mutants at 48 hpi (Fig. 6H; 90.0 ± 12.7 vs 19.8 ± 6.9, respectively). By 72 hpi, the number of 4C4+ microglia increased slightly in wild-type retinas, although not significantly and with more variability (95.0 ± 36.7). Although the number of 4C4+ cells increased in *irf8* mutants between 48 and 72 hpi (19.8 ± 6.9 vs. 31.33 ± 18.14), the overall increase was not considered statistically significant and there were far fewer 4C4+ microglia were observed in *irf8* mutants compared to wild-type. When comparing the overall increase between 24 and 72 hpi, the increase in 4C4+ microglia within the SRS was considered statistically significant and was approximately 2.5-fold (12.5 ± 5.6 vs 31.3 ± 18.1; $p < 0.05$). While the number of microglia in both wild-type and *irf8* mutant retinas increased by 2- to 2.5-fold following injury, the increase occurred within the first 48 hpi in wild-type retinas compared to the slower increase observed in *irf8* mutants. The 4C4+ microglia in *irf8* mutants did, however, adopt ameboid morphologies in response to photoreceptor damage. This suggested that these microglia retained at least partial function. To determine if 4C4+ microglia were proliferating, the percentage of EdU+ cells that were also 4C4+ (i.e. EdU+/4C4+) cells was quantified at each time point. With only 0–1 cell on average labeling with EdU in the SRS at 24 hpi, each section contained either a 100% EdU+/4C4+ cells or 0% EdU+/4C4+ cells, resulting in a binary distribution (Fig. 6I). At 48 hpi, more than 96% of all EdU+ cells were 4C4+ in wild-type retinas, whereas only 83.9% of EdU+ cells were 4C4+ in *irf8* mutants. By 72 hpi, the percentage of EdU+/4C4+ cells remained at $92.0 \pm 7.8\%$ in wild-type retinas but had declined to $66.3 \pm 24.5\%$ in *irf8* mutants. In other words, *irf8* mutants had a lower percentage of EdU+/4C4+ cells (Fig. 6I) than wild-type animals after injury and far fewer 4C4+ cells overall than wild-type animals (Fig. 6H). Collectively, these data support several findings. First, 4C4+ microglia respond rapidly to light damage and mobilize to the SRS in wild-type retinas but do not proliferate within the first 24 h post injury. Second, microglia proliferate in response to damage sometime between 24–48 hpi and continue to proliferate and accumulate at the site of damage through 72 hpi. Importantly, more than 90% of all EdU+ cells were 4C4+ (Fig. 6I), indicating that microglia are the most abundant proliferating cell population in

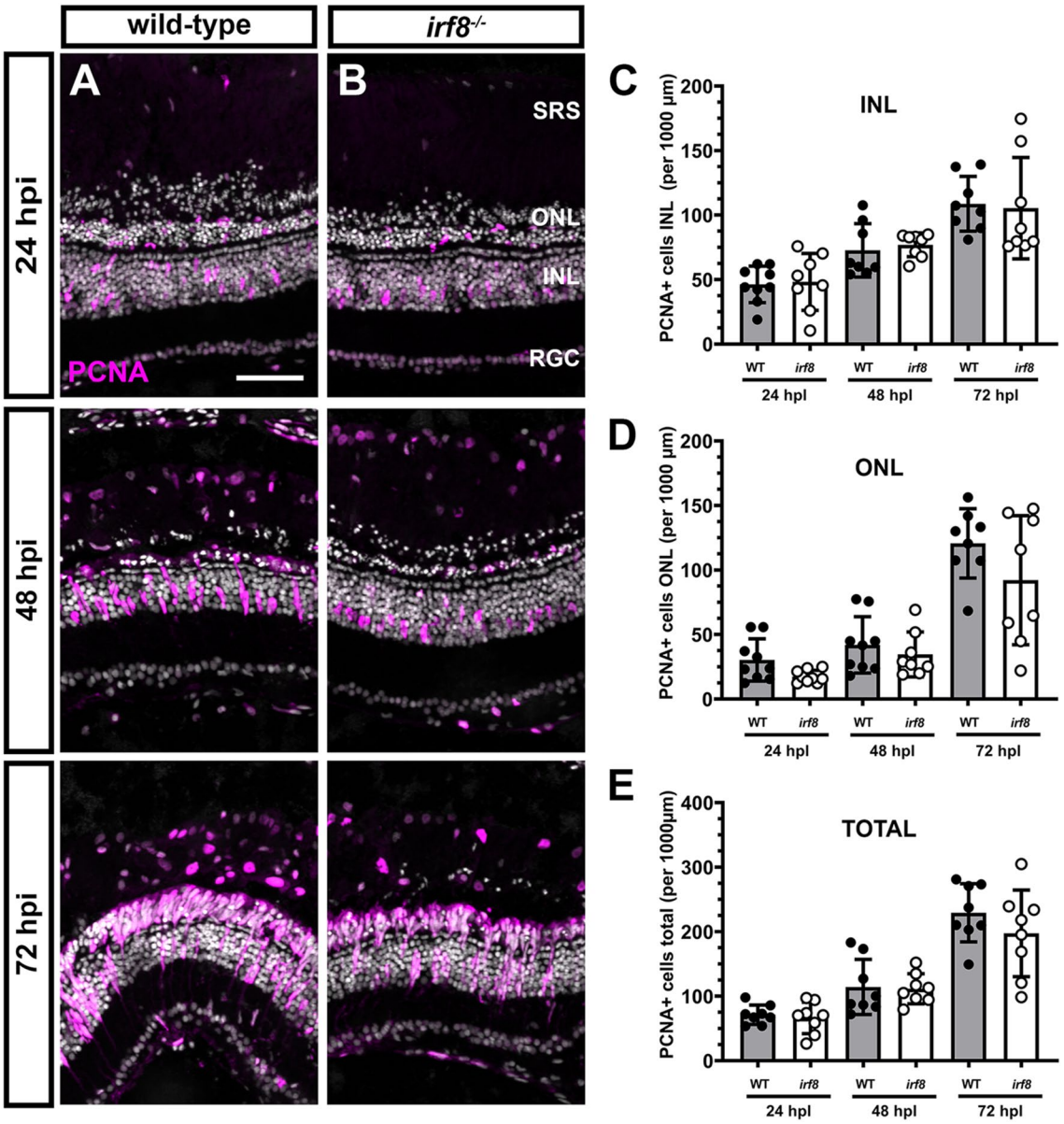

Fig. 4. Light damage induces proliferation of Müller glia and generation of neural progenitors in *irf8* mutants. (**A**,**B**) Immunohistochemistry with anti-PCNA antibodies (magenta) on retinal cryosections from 6 mpf wild-type and *irf8* mutants at 24, 48, and 72 h post light injury (hpi). At 24 hpi, proliferating Müller glia are seen in the INL of both wild-type and *irf8* mutants. At 48 hpi, clusters of neurogenic progenitors appear and by 72 hpi these clusters continue to proliferate and have migrated to the ONL of both wild-type and *irf8* mutants. (**C**–**E**) Quantification of PCNA+ cell density in the INL and ONL and total density of PCNA+ cells in the dorsal retinas of wild-type and *irf8* mutants at times after light damage. No statistical difference was found between wild-type and *irf8* mutants at any time point. Data are plotted as means ± SD and individual points represent data from one retina (n = 10–13). Wild-type and *irf8* data were compared by unpaired Welch's *t*-tests for individual time points. No statistical difference was observed between any groups. *SRS* subretinal space, *ONL* outer nuclear layer, *INL* inner nuclear layer, *RGC* retinal ganglion cell layer. Scale bar, 50 µm.

the SRS. In contrast, the limited number of 4C4+ cells in *irf8* mutants showed limited capacity for proliferation. Although the percentage of EdU+/4C4+ cells in the *irf8* mutants was >66% (Fig. 6I), the absolute number of EdU+ cells remained small (Fig. 6G). From this, we conclude that light damage of *irf8* mutants does not induce a significant increase of 4C4+ microglia via proliferation and that the robust regenerative response from Müller glia does not correlate with microglia proliferation in *irf8* mutants.

Light-induced photoreceptor death does not damage the blood-retinal-barrier (BRB)

We next asked whether acute light injury could disrupt the blood-retinal-barrier (BRB) and allow access to circulating factors that respond to damage and induce Müller glia proliferation. In mammalian models of retinal degeneration, infiltrating monocytes enter the retina from the intraretinal vasculature but not the choroid[37].

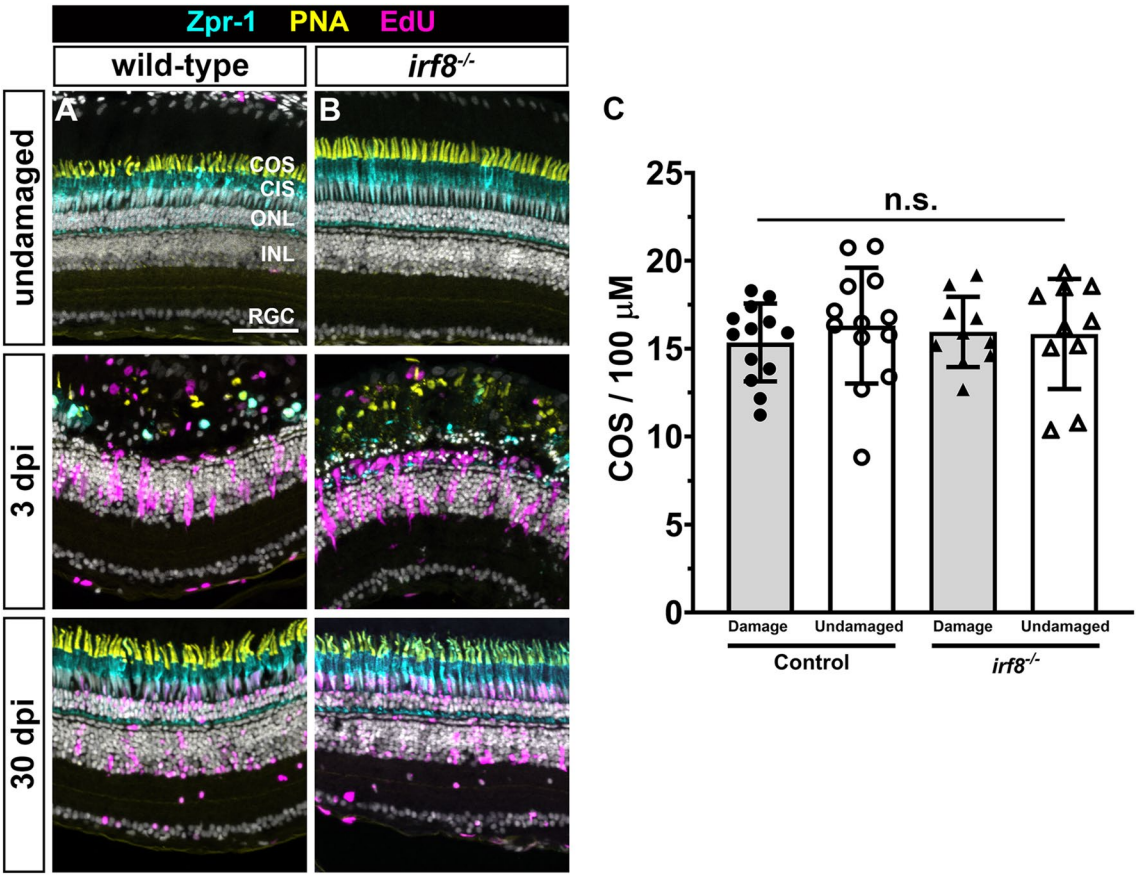

Fig. 5. Photoreceptors regenerate in *irf8* mutants following acute light damage. (**A**,**B**) Immunohistochemistry with Zpr1 (cyan), PNA (yellow), and EdU (magenta) on retinal cryosections from undamaged wild-type and *irf8* mutants (top row) and at 3 days post injury (dpi; middle row) or 30 dpi (bottom row). Light damage fully ablated cones in the central region of the dorsal retina at 3 dpi and photoreceptors regenerated by 30 dpi. (**C**) Quantification of cone outer segment density in damaged and undamaged areas of the retina. Data are plotted as means ± SD and individual points represent data from one retina (n = 8–9). Data were analyzed by Welch's ANOVA test with Dunnett T3 correction for multiple comparisons. No statistical difference was observed between any groups. *COS* cone outer segments, *CIS* cone inner segments, *ONL* outer nuclear layer, *INL* inner nuclear layer, *RGC* retinal ganglion cell layer. Scale bar, 50 µm.

Zebrafish lack this intraretinal vasculature and, therefore, the choroid or hyaloid vasculature represent the only potential source of circulating monocytes. To test the effect of light damage on BRB maintenance, we conducted light damage experiments on *Tg*(*l-fabp:DBP-EGFP*) transgenic zebrafish. This transgenic line expresses a EGFP-tagged vitamin D binding protein in blood plasma, thereby permitting visualization of BRB integrity in vivo using fluorescence microscopy or confocal scanning laser ophthalmoscopy (cSLO)[29,32]. Imaging with cSLO allows repeated imaging of zebrafish vasculature in the same animal across multiple time points. In DMSO-treated control fish, the BRB remained intact over a period of 48 h of imaging (Fig. 7A). Retinoid acid signaling is necessary for the maintenance of the BRB[31]. To demonstrate the use of cSLO to visualize BRB breakdown, animals were treated with DEAB, an antagonist of retinaldehyde dehydrogenase (RALDH), and subsequently imaged at multiple time points over two consecutive days. The extravascular space (EVS) mean signal intensity of GFP was quantified at each time point and was found to increase significantly by 24 h (Fig. 7D). DEAB treatment resulted in BRB breakdown and leakage of EGFP into the retina within 24 h of treatment (Fig. 7B,D). Following light damage, no leakage of GFP into the retina was observed in *Tg*(*l-fabp:DBP-EGFP*) transgenic zebrafish (Fig. 7C) and the mean GFP signal intensity was not statistically different from DMSO-control fish (Fig. 7D). Consistent with these findings, all L-plastin+ cells observed in the retina following light damage were also 4C4+ (Supplemental Fig. 1). This strongly suggests that microglia are the only L-plastin+ macrophage population found in the zebrafish retina following light damage. As light damage can induce Müller glia proliferation within 24 hpi and no changes in BRB integrity are observed by 48 hpi, these results strongly suggest that light damage does not compromise the BRB. Thus, the proliferation of Müller glia in *irf8* mutants likely does not result from the infiltration of immune cells to the retina following light-damage induced vasculature injury.

To confirm that localized cell death was sufficient to induce Müller glia driven regeneration, we asked whether *irf8* mutants were responsive to the selective ablation of rod photoreceptors using the *Tg*(*rho:YFP-NTR*) transgenic line[24]. This line expresses a YFP-nitroreductase fusion protein specifically in rod photoreceptors, thereby permitting the selective death of rods upon exposure to metronidazole (MTZ). Adult zebrafish (6 mpf) were

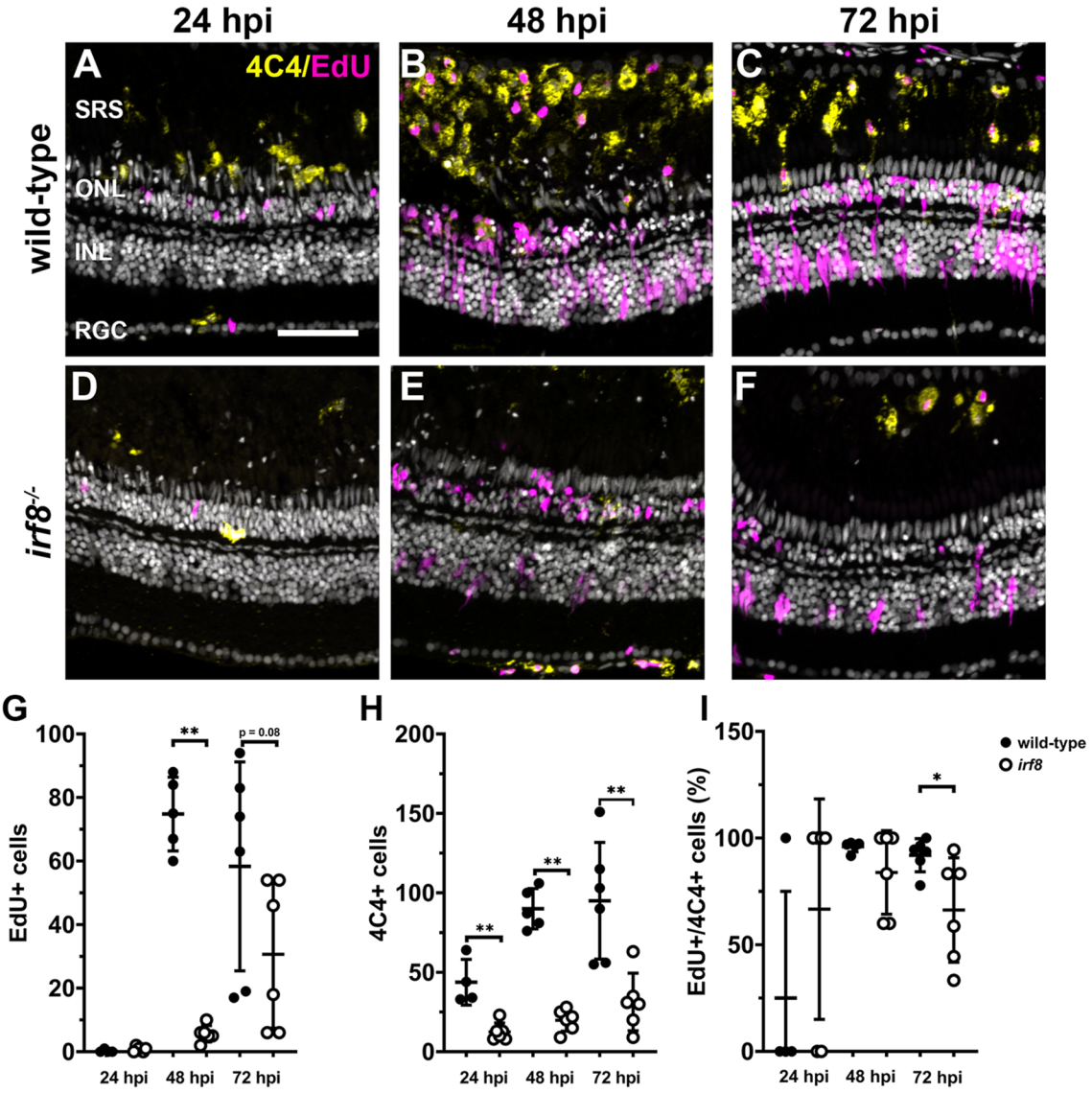

Fig. 6. Light damage does not induce microglia proliferation in *irf8* mutants. (**A**–**F**) Immunohistochemistry with EdU (magenta) to label proliferating cells and 4C4 (yellow) to label microglia/macrophages on retinal cryosections from wild-type and *irf8* mutants at 24, 48, and 72 h post injury (hpi). (**G**) Quantification of EdU+ cells in the SRS at times after light damage. (**H**) Quantification of 4C4+ cells in the SRS at times after light damage. (**I**) The ratio of Edu+/4C4+ cells within the SRS was calculated for each time point after light damage. *SRS* subretinal space, *ONL* outer nuclear layer, *INL* inner nuclear layer, *RGC* retinal ganglion cell layer. Scale bar, 50 µm.

immersed in 10 mM MTZ for ~24 h to induce rod ablation and subsequently injected with EdU to label proliferating cells. Fish allowed to recover for either 48 h or up to 30 days (Fig. 8A). At 48 h of recovery, immunohistochemistry with anti-GFP antibodies, which detected the YFP-NTR fusion protein, showed that rod photoreceptors were almost completely ablated, with only fragments of YFP+ nuclei and outer segments present in the ONL (Fig. 8B). Importantly, EdU staining identified proliferating Müller glia in both wild-type and *irf8* mutants. By 30 dpf, regenerated rods had fully repopulated the ONL in both wild-type and *irf8* mutants (Fig. 8C).

To characterize the molecular inflammatory response to light damage in *irf8* mutants, qPCR was used to assess several inflammatory genes (Fig. 9). The expression of *matrix metalloproteinase 9* (*mmp-9*), *chemokine ligand 8a* (*cxcl8*, also known as *il8*), *tumor necrosis factor b* (*tnfβ*), *interleukin 1 beta* (*il1b*), *purinergic receptor P2Y12* (*p2ry12*), and *interleukin 10* (*il-10*) were previously demonstrated to rapidly increase following NMDA and/or light damage[8,11,38]. Whereas *mmp-9* expression is specific to Müller glia[8,38] and *p2ry12* is expressed in macrophages and/or microglia[39], *il8*, *tnfβ*, and *il1b* are expressed in multiple cell types, including the RPE and endothelial cells. Similar to prior studies[8,11], we found that expression of *mmp-9*, *il8*, *tnfβ*, and *il10* increased significantly after light damage in both wild-type and *irf8* mutants (Fig. 9). Expression of *mmp-9* and *tnfβ* peaked between 48–72 hpi in both wild-type and *irf8* mutants. Interestingly, the expression of *il8* was significantly higher in *irf8* mutants than wild-type siblings at 6 hpi, when expression of *il8* peaks. Only a modest increase in the

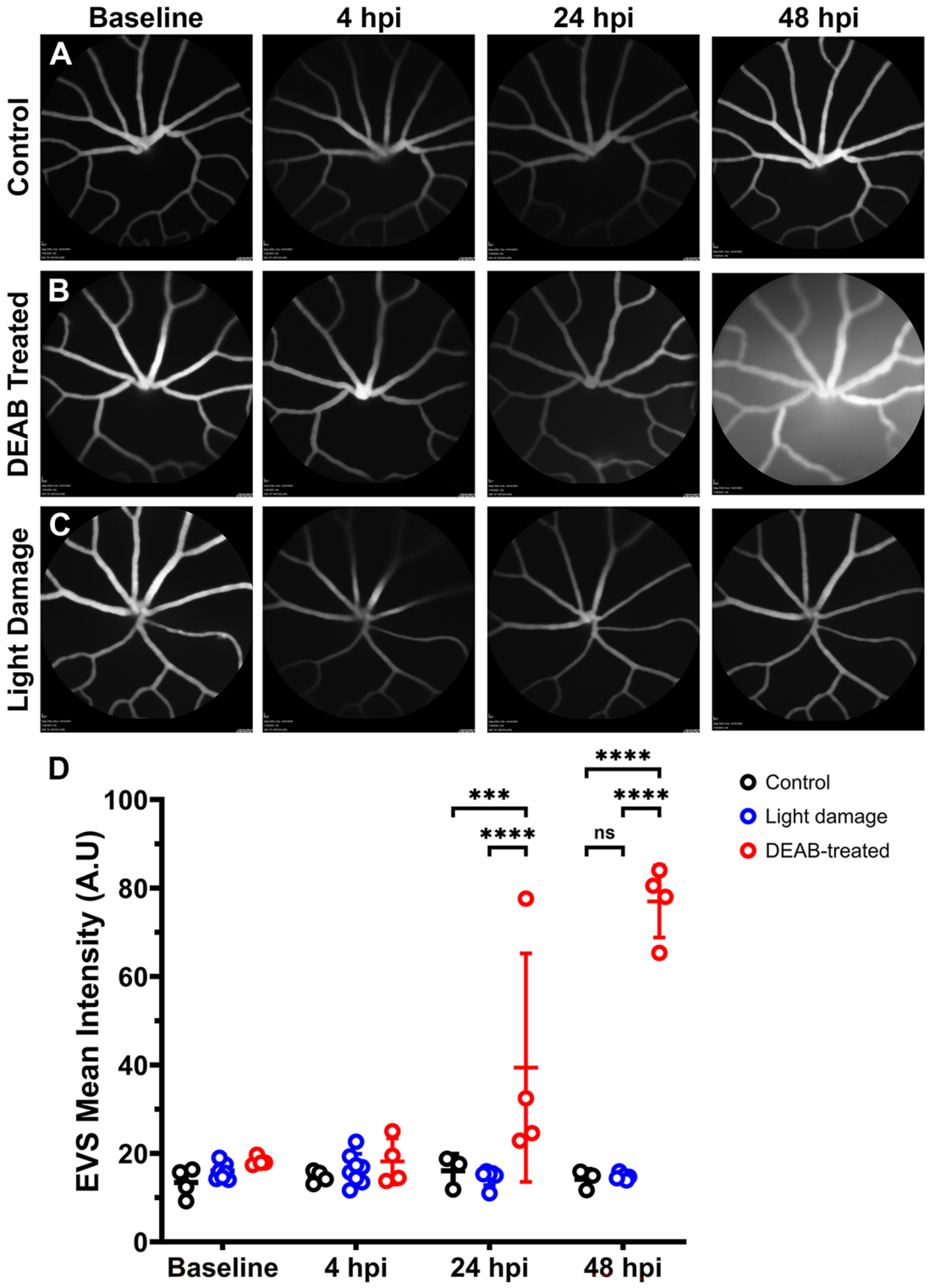

Fig. 7. Light damage does not disrupt the blood-retinal-barrier. (**A**–**C**) Longitudinal confocal scanning laser ophthalmoscopy (cSLO) images from 6 mpf *Tg*(*l-fabp:DBP-eGFP*) zebrafish before and at 4–48 h after treatment with DMSO, DEAB, or with light damage. (**D**) Quantification of extravascular space (EVS) mean signal intensity determined from cSLO images at different time points after treatment. Data were analyzed with a two-way ANOVA with Tukey's correction for multiple comparisons. ***$p < 0.0005$; ****$p < 0.0001$.

expression of *il1b* and *il10* was observed in wild-type animals and *irf8* mutants, with no statistical differences between wild-type or *irf8* mutants. Surprisingly, we did not see any significant change in expression of *p2ry12*

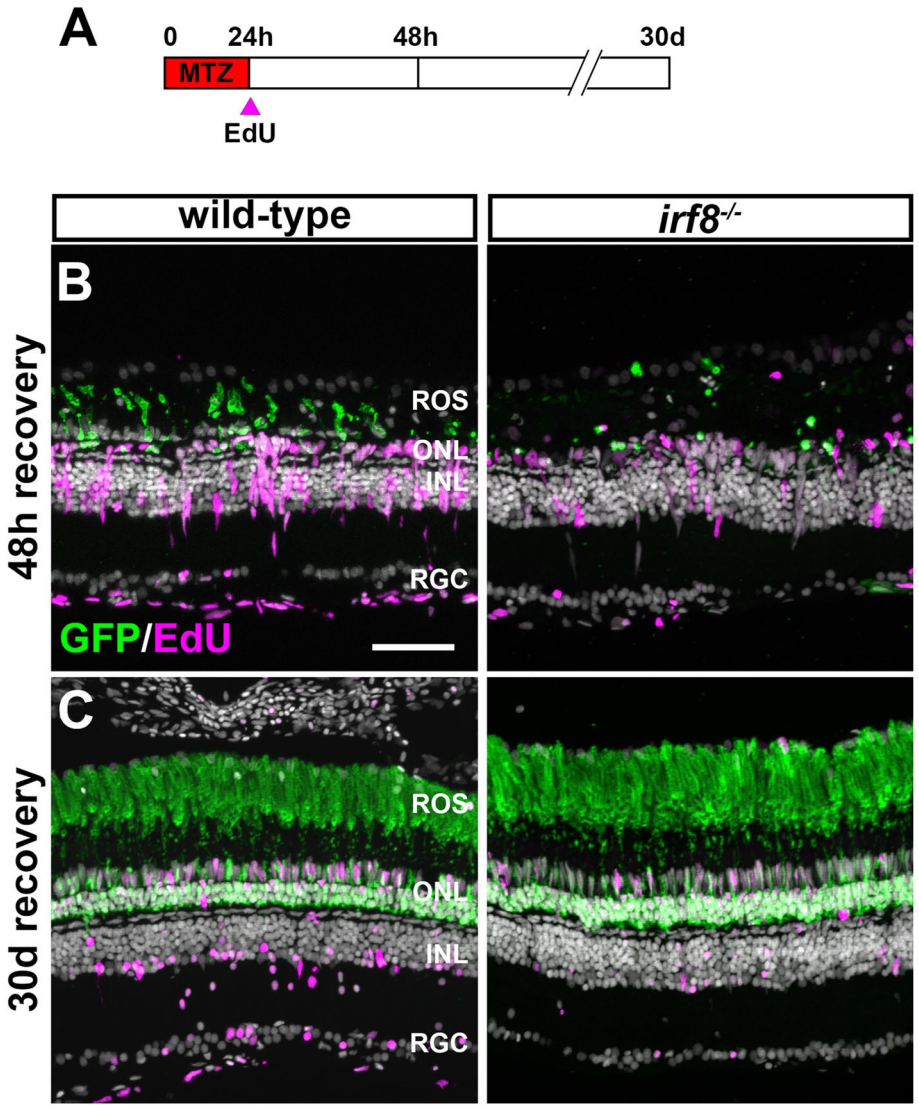

Fig. 8. Regeneration after metronidazole-induced rod ablation in *irf8;Tg*(*zOPS:ntrB-EGFP*)*gm500* animals. (**A**) Schematic illustrating experimental paradigm and treatment regimen. (**B**,**C**) Immunohistochemistry with anti-GFP antibodies (green) and EdU (magenta) on retinal cryosections from wild-type and *irf8* mutants at 48 h post MTZ treatment or 30 days post MTZ treatment. MTZ treatment fully ablated rod photoreceptors and induced Müller glia proliferation at 48 h post treatment and rod fully regenerated by 30 dpi. *ROS* rod outer segments, *ONL* outer nuclear layer, *INL* inner nuclear layer, *RGC* retinal ganglion cell layer. Scale bar, 50 µm.

following light damage to either wild-type or *irf8* mutants, although this gene was previously shown to increase following NMDA damage[11]. These results indicate that damage induces expression of several pro-inflammatory cytokines even in microglia-deficient retinas.

Discussion

Inflammatory signaling represents a crucial step in initiating retinal regeneration in zebrafish. Both acute and chronic degeneration of retinal neurons triggers a robust inflammatory response characterized by the accumulation of microglia/macrophages to the site of the lesion and within the subretinal space[10,11,30,40]. This microglial response correlates with the release of pro-inflammatory factors that bind receptors on Müller glia and activate intracellular signaling pathways that result in Müller glia reprogramming[2]. Indeed, microglia in regenerating retinas express several pro-inflammatory genes known to promote regeneration[9]. While the cellular and molecular response of microglia to retina injury has attracted significant attention, the necessity of microglia to retinal regeneration remains unclear. We investigated retina regeneration in *irf8* mutant zebrafish, which have a significant depletion of retinal microglia. We showed that acute injury induced proliferation of Müller glia and neuronal progenitors in *irf8* mutants and led to the transcriptional upregulation of several known pro-inflammatory cytokines at levels that matched or even exceeded that observed in wild-type animals.

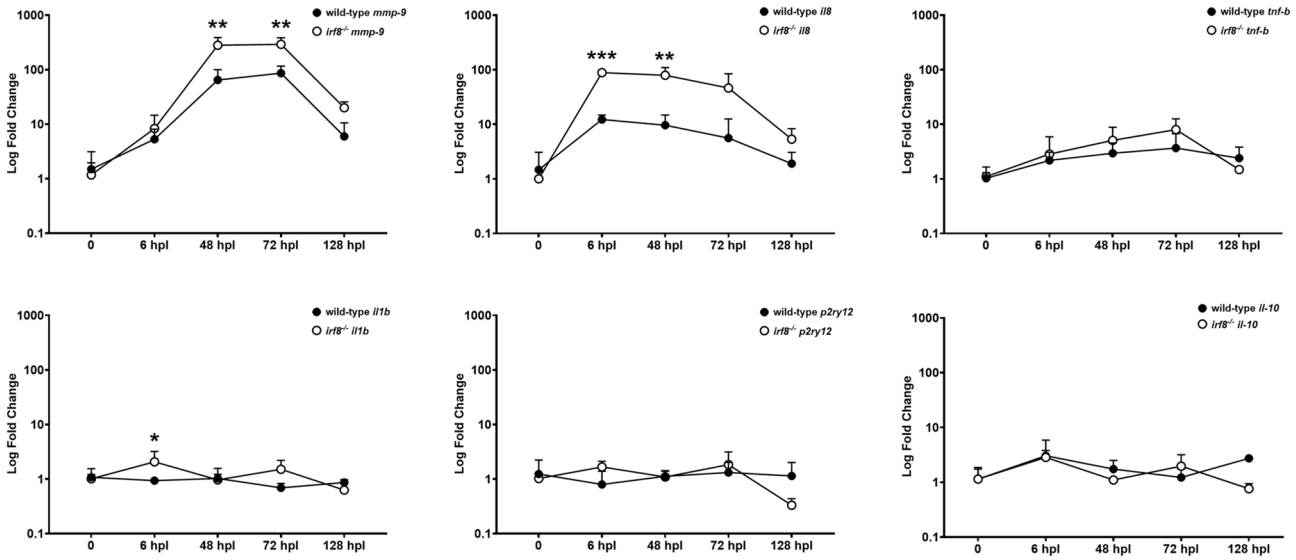

Fig. 9. Dynamics of inflammatory signaling following light damage in 6 mpf *irf8* mutants and wild-type siblings. The change in gene expression of inflammatory genes following light damage is plotted as a function of time after damage to wild-type or *irf8* mutants. Expression is represented as the log fold change calculated using the ddC_t method and compared against gene expression in undamaged retinas. $^{***}p < 0.0005$; $^{**}p < 0.01$; $^{*}p < 0.05$.

Prior to our studies, several lines of evidence suggested that microglia mediated inflammation was necessary for Müller glia reprogramming and retinal regeneration. Multiple groups have used dexamethasone to suppress inflammatory signaling and observed a concomitant reduction in Müller glia proliferation and total microglia[10–12,24]. Treatment with the CSF1R inhibitor, PLX3397, before and following laser-mediated photoreceptor ablation resulted in depletion of retina microglia and prevented regeneration of the outer nuclear layer[23]. Utilizing a genetic approach, Zhang and colleagues used the *mpeg1* promoter to drive expression of a nitroreductase-mCherry fusion protein specifically in microglia and macrophages and ablate those cells prior to retinal injury. This significantly suppressed Müller glia reprogramming following a needle-poke injury[12]. In contrast, we report that regeneration occurs normally in *irf8* mutants with significantly reduced numbers of microglia. Several reasons could potentially explain these apparently conflicting results.

One possibility is that only a small number of microglia are sufficient to produce an inflammatory response capable of inducing Müller glia reprogramming and proliferation. While the *irf8* mutants completely lack microglia during larval stages[27] a small number of partially recovered 4C4+ microglia can be seen in adult *irf8* mutants (Fig. 1). The source of these microglia is unclear, but they have phenotypes consistent with macrophages[41] and likely develop independent of *irf8*. In response to damage, however, the 4C4+ cells found in *irf8* mutants do not re-enter the cell cycle and proliferate in number in the same manner as wild-type 4C4+ cells (this study and[40]). This suggests that the 4C4+ cells in *irf8* mutants may not exhibit a normal inflammatory response to acute injury. We cannot, however, completely exclude the possibility that the remaining 4C4+ cells are sufficient for regeneration in the zebrafish *irf8* adult retina.

A second possibility is that other cells compensate for the drastic reduction of microglia in *irf8* mutants. Müller glia[38], photoreceptors[6], and the RPE[42,43] all release pro-inflammatory cytokines in response to injury. Damage to photoreceptors triggers release of TNFα and Mmp-9 is exclusively released by Müller glia and Müller glia-derived progenitors[8]. Under wild-type conditions, paracrine signaling from microglia most certainly contributes to the pro-inflammatory response of photoreceptors and Müller glia; however, these cells are also capable of autonomously secreting cytokines that can induce regeneration[44,45]. We observed a significant increase in expression of *mmp-9*, *il8*, and *tnfb*, in both wild-type and *irf8* mutant retinas, suggesting that other cells continue to mount a robust pro-inflammatory response even with a substantial reduction in microglia. In *irf8* mutant larvae, the Müller glia compensate for the loss of microglia by engulfing dying cells and increasing phagocytic load[46]. It is not entirely surprising that a compensation mechanism exists in an attempt to maintain retinal homeostasis.

Genetic approaches that block the formation of microglia (e.g. *irf8* mutations) and transgene-mediated ablation of microglia[12] may differ from pharmacological-depletion of microglia[23]. Blocking microglia differentiation during development or eliminating microglia in younger animals could result in chronic changes to retinal homeostasis in the adult retina. For example, tamoxifen-induced depletion of microglia in the retinas of young adult mice resulted in altered synaptic architecture and reduced visual function without changing overall retinal structure[15]. Interestingly, microglia-depleted animals exhibited a small, but significant increase (1.3- to 1.6-fold) in expression of markers associated with Müller glia gliosis and astrocyte activation. We found that zebrafish *irf8* mutants exhibited cone photoreceptor loss in older animals. These results indicate that microglia play important roles in maintaining retinal physiology. The chronic absence or reduction in microglia could induce a gliotic response that is associated with regeneration in zebrafish. In contrast, pharmacological agents that broadly suppress inflammation (e.g. dexamethasone) or ablate microglia may also have secondary effects beyond microglia.

Extended administration of CSF1R inhibitors commonly used to deplete microglia (e.g. PLX3397) was shown to have deleterious off-target effects on neural progenitor cells[47] and mature myeloid cells in the circulation and bone marrow, some cells of which do not express CSF1R[48]. The failure to regenerate photoreceptors following laser injury in PLX3397-treated animals may reflect an impact on Müller -glia derived progenitor cell proliferation within the inner nuclear layer in addition to the depletion of microglia.

In conclusion, we show that photoreceptor regeneration occurs in zebrafish *irf8* mutants following light damage. The *irf8* mutants have normal retinal architecture up through 6 mpf and then undergo a slow cone degeneration by 10 mpf. Expression of pro-inflammatory cytokines occurs normally within the retinas of *irf8* mutants. Proper regeneration in zebrafish requires an initial pro-inflammatory signaling response following an injury and multiple cell types, including microglia, serve as the source of those pro-inflammatory molecules. The results of this study should not be interpreted that microglia do not participate in the inflammatory response or regeneration. Studies clearly indicate that microglia migrate to the source of damage and express factors associated with regeneration[9,38,40]. Differing conclusions regarding the role of microglia likely reflect differences in genetic background and/or methodologies for blocking or ablation microglia function, dosing and pharmacokinetics of various drugs, and even injury paradigms. As such, caution is warranted when comparing and interpreting results from studies that use different approaches. Additional work is needed to determine if the *irf8* mutant represents an ideal model for assessing microglia absence on neural regeneration in adult zebrafish.

Data availability

All data is provided within the manuscript or supplementary information. The datasets used and/or analyzed during the current study are available from the corresponding author on reasonable request.

Received: 28 June 2024; Accepted: 21 August 2024
Published online: 30 August 2024

References

1. Goldman, D. Muller glial cell reprogramming and retina regeneration. *Nat. Rev. Neurosci.* **15**, 431–442. https://doi.org/10.1038/nrn3723 (2014).
2. Nagashima, M. & Hitchcock, P. F. Inflammation regulates the multi-step process of retinal regeneration in zebrafish. *Cells* https://doi.org/10.3390/cells10040783 (2021).
3. Gao, H., Luodan, A., Huang, X., Chen, X. & Xu, H. Muller glia-mediated retinal regeneration. *Mol. Neurobiol.* **58**, 2342–2361. https://doi.org/10.1007/s12035-020-02274-w (2021).
4. Nagashima, M., Barthel, L. K. & Raymond, P. A. A self-renewing division of zebrafish Muller glial cells generates neuronal progenitors that require N-cadherin to regenerate retinal neurons. *Development* **140**, 4510–4521. https://doi.org/10.1242/dev.090738 (2013).
5. Lahne, M., Nagashima, M., Hyde, D. R. & Hitchcock, P. F. Reprogramming muller glia to regenerate retinal neurons. *Annu. Rev. Vis. Sci.* **6**, 171–193. https://doi.org/10.1146/annurev-vision-121219-081808 (2020).
6. Nelson, C. M. *et al.* Tumor necrosis factor-alpha is produced by dying retinal neurons and is required for Muller glia proliferation during zebrafish retinal regeneration. *J. Neurosci.* **33**, 6524–6539. https://doi.org/10.1523/JNEUROSCI.3838-12.2013 (2013).
7. Zhao, X. F. *et al.* Leptin and IL-6 family cytokines synergize to stimulate Muller glia reprogramming and retina regeneration. *Cell Rep.* **9**, 272–284. https://doi.org/10.1016/j.celrep.2014.08.047 (2014).
8. Silva, N. J. *et al.* Inflammation and matrix metalloproteinase 9 (Mmp-9) regulate photoreceptor regeneration in adult zebrafish. *Glia* **68**, 1445–1465. https://doi.org/10.1002/glia.23792 (2020).
9. Mitchell, D. M., Sun, C., Hunter, S. S., New, D. D. & Stenkamp, D. L. Regeneration associated transcriptional signature of retinal microglia and macrophages. *Sci. Rep.* **9**, 4768. https://doi.org/10.1038/s41598-019-41298-8 (2019).
10. Fogerty, J. *et al.* Notch inhibition promotes regeneration and immunosuppression supports cone survival in a zebrafish model of inherited retinal dystrophy. *J. Neurosci.* https://doi.org/10.1523/JNEUROSCI.0244-22.2022 (2022).
11. Iribarne, M. & Hyde, D. R. Different inflammation responses modulate Muller glia proliferation in the acute or chronically damaged zebrafish retina. *Front. Cell Dev. Biol.* **10**, 892271. https://doi.org/10.3389/fcell.2022.892271 (2022).
12. Zhang, Z. *et al.* Inflammation-induced mammalian target of rapamycin signaling is essential for retina regeneration. *Glia* **68**, 111–127. https://doi.org/10.1002/glia.23707 (2020).
13. Silverman, S. M. & Wong, W. T. Microglia in the retina: Roles in development, maturity, and disease. *Annu. Rev. Vis. Sci.* **4**, 45–77. https://doi.org/10.1146/annurev-vision-091517-034425 (2018).
14. O'Koren, E. G. *et al.* microglial function is distinct in different anatomical locations during retinal homeostasis and degeneration. *Immunity* **50**, 723-737 e727. https://doi.org/10.1016/j.immuni.2019.02.007 (2019).
15. Wang, X. *et al.* Requirement for microglia for the maintenance of synaptic function and integrity in the mature retina. *J. Neurosci.* **36**, 2827–2842. https://doi.org/10.1523/JNEUROSCI.3575-15.2016 (2016).
16. Hickman, S., Izzy, S., Sen, P., Morsett, L. & El Khoury, J. Microglia in neurodegeneration. *Nature neuroscience* **21**, 1359–1369. https://doi.org/10.1038/s41593-018-0242-x (2018).
17. Paolicelli, R. C. *et al.* Microglia states and nomenclature: A field at its crossroads. *Neuron* **110**, 3458–3483. https://doi.org/10.1016/j.neuron.2022.10.020 (2022).
18. Gao, C., Jiang, J., Tan, Y. & Chen, S. Microglia in neurodegenerative diseases: Mechanism and potential therapeutic targets. *Signal Transduct. Target. Ther.* **8**, 359. https://doi.org/10.1038/s41392-023-01588-0 (2023).
19. Gupta, N., Brown, K. E. & Milam, A. H. Activated microglia in human retinitis pigmentosa, late-onset retinal degeneration, and age-related macular degeneration. *Exp. Eye Res.* **76**, 463–471. https://doi.org/10.1016/s0014-4835(02)00332-9 (2003).
20. Amor, S. *et al.* Inflammation in neurodegenerative diseases—An update. *Immunology* **142**, 151–166. https://doi.org/10.1111/imm.12233 (2014).
21. Kyritsis, N. *et al.* Acute inflammation initiates the regenerative response in the adult zebrafish brain. *Science* **338**, 1353–1356. https://doi.org/10.1126/science.1228773 (2012).
22. Kizil, C., Kyritsis, N. & Brand, M. Effects of inflammation on stem cells: Together they strive?. *EMBO Rep.* **16**, 416–426. https://doi.org/10.15252/embr.201439702 (2015).
23. Conedera, F. M., Pousa, A. M. Q., Mercader, N., Tschopp, M. & Enzmann, V. Retinal microglia signaling affects Muller cell behavior in the zebrafish following laser injury induction. *Glia* **67**, 1150–1166. https://doi.org/10.1002/glia.23601 (2019).
24. White, D. T. *et al.* Immunomodulation-accelerated neuronal regeneration following selective rod photoreceptor cell ablation in the zebrafish retina. *Proc. Natl. Acad. Sci. USA* **114**, E3719–E3728. https://doi.org/10.1073/pnas.1617721114 (2017).

25. Todd, L., Finkbeiner, C., Wong, C. K., Hooper, M. J. & Reh, T. A. Microglia suppress Ascl1-induced retinal regeneration in mice. *Cell Rep.* **33**, 108507. https://doi.org/10.1016/j.celrep.2020.108507 (2020).
26. Shiau, C. E., Kaufman, Z., Meireles, A. M. & Talbot, W. S. Differential requirement for irf8 in formation of embryonic and adult macrophages in zebrafish. *PLoS One* **10**, e0117513. https://doi.org/10.1371/journal.pone.0117513 (2015).
27. Earley, A. M., Graves, C. L. & Shiau, C. E. Critical role for a subset of intestinal macrophages in shaping gut microbiota in adult zebrafish. *Cell Rep.* **25**, 424–436. https://doi.org/10.1016/j.celrep.2018.09.025 (2018).
28. White, D. T. & Mumm, J. S. The nitroreductase system of inducible targeted ablation facilitates cell-specific regenerative studies in zebrafish. *Methods* **62**, 232–240. https://doi.org/10.1016/j.ymeth.2013.03.017 (2013).
29. Xie, J., Farage, E., Sugimoto, M. & Anand-Apte, B. A novel transgenic zebrafish model for blood-brain and blood-retinal barrier development. *BMC Dev. Biol.* **10**, 76. https://doi.org/10.1186/1471-213X-10-76 (2010).
30. Song, P., Fogerty, J., Cianciolo, L. T., Stupay, R. & Perkins, B. D. Cone Photoreceptor degeneration and neuroinflammation in the zebrafish Bardet-Biedl syndrome 2 (bbs2) mutant does not lead to retinal regeneration. *Front. Cell Dev. Biol.* **8**, 578528. https://doi.org/10.3389/fcell.2020.578528 (2020).
31. Pollock, L. M., Xie, J., Bell, B. A. & Anand-Apte, B. Retinoic acid signaling is essential for maintenance of the blood-retinal barrier. *FASEB J.* **32**, 5674–5684. https://doi.org/10.1096/fj.201701469R (2018).
32. Bell, B. A. *et al.* Retinal vasculature of adult zebrafish: In vivo imaging using confocal scanning laser ophthalmoscopy. *Exp. Eye Res.* **129**, 107–118. https://doi.org/10.1016/j.exer.2014.10.018 (2014).
33. Bell, B. A. *et al.* The adult zebrafish retina: In vivo optical sectioning with confocal scanning laser ophthalmoscopy and spectral-domain optical coherence tomography. *Exp. Eye Res.* https://doi.org/10.1016/j.exer.2016.10.001 (2016).
34. Rovira, M. *et al.* Zebrafish Galectin 3 binding protein is the target antigen of the microglial 4C4 monoclonal antibody. *Dev. Dyn.* https://doi.org/10.1002/dvdy.549 (2022).
35. Allison, W. T. *et al.* Ontogeny of cone photoreceptor mosaics in zebrafish. *J. Comp. Neurol.* **518**, 4182–4195. https://doi.org/10.1002/cne.22447 (2010).
36. Vihtelic, T. S., Soverly, J. E., Kassen, S. C. & Hyde, D. R. Retinal regional differences in photoreceptor cell death and regeneration in light-lesioned albino zebrafish. *Exp. Eye Res.* **82**, 558–575. https://doi.org/10.1016/j.exer.2005.08.015 (2006).
37. Karlen, S. J. *et al.* Monocyte infiltration rather than microglia proliferation dominates the early immune response to rapid photoreceptor degeneration. *J. Neuroinflammation* **15**, 344. https://doi.org/10.1186/s12974-018-1365-4 (2018).
38. Hoang, T. *et al.* Gene regulatory networks controlling vertebrate retinal regeneration. *Science* https://doi.org/10.1126/science.abb8598 (2020).
39. Cavone, L. *et al.* A unique macrophage subpopulation signals directly to progenitor cells to promote regenerative neurogenesis in the zebrafish spinal cord. *Dev. Cell* **56**, 1617-1630 e1616. https://doi.org/10.1016/j.devcel.2021.04.031 (2021).
40. Mitchell, D. M., Lovel, A. G. & Stenkamp, D. L. Dynamic changes in microglial and macrophage characteristics during degeneration and regeneration of the zebrafish retina. *J. Neuroinflammation* **15**, 163. https://doi.org/10.1186/s12974-018-1185-6 (2018).
41. Yu, T. *et al.* Distinct regulatory networks control the development of macrophages of different origins in zebrafish. *Blood* **129**, 509–519. https://doi.org/10.1182/blood-2016-07-727651 (2017).
42. Greene, W. A., Burke, T. A., Por, E. D., Kaini, R. R. & Wang, H. C. Secretion profile of induced pluripotent stem cell-derived retinal pigment epithelium during wound healing. *Investig. Ophthalmol. Vis. Sci.* **57**, 4428–4441. https://doi.org/10.1167/iovs.16-19192 (2016).
43. Holtkamp, G. M. *et al.* Polarized secretion of IL-6 and IL-8 by human retinal pigment epithelial cells. *Clin. Exp. Immunol.* **112**, 34–43. https://doi.org/10.1046/j.1365-2249.1998.00560.x (1998).
44. Schmalen, A. *et al.* Proteomic phenotyping of stimulated Muller cells uncovers profound pro-inflammatory signaling and antigen-presenting capacity. *Front. Pharmacol.* **12**, 771571. https://doi.org/10.3389/fphar.2021.771571 (2021).
45. Giblin, M. J. *et al.* Nuclear factor of activated T-cells (NFAT) regulation of IL-1beta-induced retinal vascular inflammation. *Biochim. Biophys. Acta Mol. Basis Dis.* **1867**, 166238. https://doi.org/10.1016/j.bbadis.2021.166238 (2021).
46. Thiel, W. A., Blume, Z. I. & Mitchell, D. M. Compensatory engulfment and Muller glia reactivity in the absence of microglia. *Glia* **70**, 1402–1425. https://doi.org/10.1002/glia.24182 (2022).
47. Liu, Y. *et al.* Concentration-dependent effects of CSF1R inhibitors on oligodendrocyte progenitor cells ex vivo and in vivo. *Exp. Neurol.* **318**, 32–41. https://doi.org/10.1016/j.expneurol.2019.04.011 (2019).
48. Claeys, W. *et al.* Limitations of PLX3397 as a microglial investigational tool: Peripheral and off-target effects dictate the response to inflammation. *Front. Immunol.* **14**, 1283711. https://doi.org/10.3389/fimmu.2023.1283711 (2023).

Acknowledgements

The authors thank Sarah Grabinski (Cleveland Clinic) for technical assistance and the staff of the Biological Resources Unit (BRU) in the Lerner Research Institute at the Cleveland Clinic for animal care. This work was supported by U.S. National Institutes of Health, National Eye Institute (NEI) grants R01EY030574 and R01EY034755 (B.D.P), 1R01EY02618 (B.A.A.), and T32EY024236 and P30EY025585 Grants to Cole Eye Institute; a Research to Prevent Blindness Unrestricted/Challenge Grant; and a Foundation Fighting Blindness Center Grant.

Author contributions

PS: experimental procedures, data analysis; DP: experimental procedures, data analysis; RS: experimental procedures, data analysis; LMP: experimental procedures; BAA: experimental design; BDP: concept, design, experimental procedures, data analysis. BDP prepared all figures and wrote the manuscript. All authors read and approved the final manuscript.

Competing interests

The authors declare no competing interests.

Additional information

Supplementary Information The online version contains supplementary material available at https://doi.org/10.1038/s41598-024-70859-9.

Correspondence and requests for materials should be addressed to B.D.P.